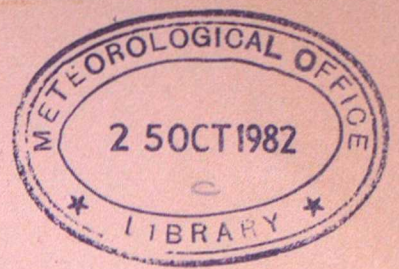


285



LONDON, METEOROLOGICAL OFFICE.

Met.O.19 Branch Memorandum No.67.

A theoretical study of the retrieval of atmospheric temperature waves from satellite radiances using regression techniques. By EYRE, J.R.

London, Met.Off., Met.O.19 Branch Mem.No.67, 1982, 31cm.Pp.10, 4 pls.5 Refs.

An unofficial document - restriction on first page to be observed.

FGZ

National Meteorological Library
and Archive

Archive copy - reference only

History Copy



138780

MET 0 19 BRANCH MEMORANDUM NO. 67

A THEORETICAL STUDY OF THE RETRIEVAL OF ATMOSPHERIC TEMPERATURE
WAVES FROM SATELLITE RADIANCES USING REGRESSION TECHNIQUES

by

EYRE J. R.

April 1982
Met 0.19
(Satellite Meteorology Branch)
Meteorological Office
London Road
Bracknell
Berkshire RG12 2SZ

NOTE: This paper has not been published. Permission to quote from it should be obtained from the Assistant Director of the above Meteorological Office branch.

A THEORETICAL STUDY OF THE RETRIEVAL OF ATMOSPHERIC TEMPERATURE WAVES FROM SATELLITE RADIANCES USING REGRESSION TECHNIQUES

1. Introduction

The global coverage given by polar-orbiting satellites offers an opportunity for detailed study of atmospheric temperature waves. However, many of the waves of interest exhibit a slope of phase with height and consequently have a vertical as well as a horizontal wavelength. It is well known that the width of the weighting functions of temperature sounding instruments leads to retrieved temperature profiles which are smoother in the vertical than the true profiles, and so it is to be expected that temperature waves with relatively short vertical wavelengths will not be retrieved or will be retrieved at lower amplitude.

To minimise such problems when studying waves it is probably best to work with the original radiances, although the waves in these are also reduced in amplitude as the vertical wavelength decreases. Hirota (1978) has approached the problem by deciding which waves he is looking for and constructing empirically a combination of weighting functions which correlates well with these waves. However it is to be expected that most researchers studying atmospheric waves will be working with retrieved fields of temperature or thickness and will not wish to be limited by a retrieval which has been tuned to resolve waves of a particular type. In fact the retrieval scheme will probably have been tuned to optimize accuracy measured by a quantity such as r.m.s. temperature difference for the whole profile.

Many studies have been made of the accuracy of temperature profiles retrieved from satellite radiances. Most have concentrated on the profile as a whole by considering the r.m.s. temperature error at different heights (e.g. Hayden, 1976) or the impact on numerical forecast (Philips, 1976) or the theoretical aspects of vertical resolution using weighting function information in the retrievals (Conrath, 1972). This study is confined to the retrieval of temperature waves by multiple linear regression, since operational retrieval schemes for TIROS-N series sounders (HIRS, MSU and SSU) currently use this technique and it may be supposed that many studies of waves will be based on such analyses. Also, because the relative success of regression techniques springs from the high correlation between temperatures at different levels, it is not obvious how such techniques will treat vertical waves in which the expected correlations may not be present.

By considering idealised weighting functions, the amplitudes of "radiance waves" produced by a sloping temperature wave have been calculated for a range of vertical wavelengths. The temperature wave retrieved from the radiances has then been calculated and compared with the true temperature wave using a range of vertical wavelengths and different assumptions about instrumental noise.

Such a technique could be of assistance to those looking for waves using the output of a retrieval system, since it shows which waves are expected to be resolved by the retrieval and could prevent false conclusions being drawn from the absence of certain types of wave in the retrieved fields.

2. A simple illustrative example

The atmospheric temperature structure in two dimensions can be described by $T(x,y)$ where x is the horizontal co-ordinate and $y = \ln(p)$, the vertical co-ordinate. The radiance measured by one channel of a vertically-sounding satellite radiometer at x is given by

$$R(x) = \int B\{\nu_0, T(x,y)\} \cdot K(y) \cdot dy \quad (1)$$

where $K(y)$ is the weighting function and ν_0 is the effective wavenumber of the channel.

This can be re-written as

$$R(x) = \int B(x,y) \cdot K(y) \cdot dy \quad (2)$$

Let us choose a Gaussian weighting function,

$$K(y) = \frac{1}{\delta\sqrt{\pi}} \exp\left\{-\frac{(y-y_0)^2}{\delta^2}\right\} \quad (3)$$

This is not physically realistic for the atmosphere but is convenient for analytic treatment and demonstrates the essential properties of more realistic weighting functions.

Also, let us choose to express a temperature wave in terms of $B(x,y)$ and in the form of a mean state (which varies only with y) and a constant amplitude wave of phase which slopes with height:

$$B(x, y) = B_0(y) + B_1 \sin(k_x x + k_y y + \phi) \quad (4)$$

From equations 2, 3 and 4:

$$R(x) = \int B_0(y) K(y) dy + \frac{B_1}{\delta \sqrt{\pi}} \int \sin(k_x x + k_y y + \phi) \exp \left\{ -\frac{(y-y_0)^2}{\delta^2} \right\} dy. \quad (5)$$

If the weighting function is positioned such that surface contributions may be neglected then, on integration,

$$R(x) = R_0 + B_1 \sin(k_x x + k_y y_0 + \phi) \exp \left\{ -\frac{k_y^2 \delta^2}{4} \right\}. \quad (6)$$

This example illustrates the way in which a sloping temperature wave creates a wave in the radiances of each channel; the wave in the x-direction is maintained with its amplitude attenuated relative to the wave in $B(x, y)$. The amplitude decreases with either a decrease in vertical wavelength or an increase in the width of the weighting function.

3. A more realistic case

A more realistic weighting function is that for a strong Elsasser band:

$$K(y) = \frac{\sqrt{2}}{\sqrt{\pi}} \frac{p}{p_0} \exp \left\{ -\frac{p^2}{2p_0^2} \right\}; \quad p = e^{-y}, \quad p_0 = e^{-y_0}. \quad (7)$$

For this study 8 such weighting functions, equally spaced in y at $y_0 = -4.5, -4, \dots, -1$, acting on a realistic temperature profile, were chosen (see figure 1). This is not amenable to analytic treatment and so was tackled numerically using the following approximations:

a. Equation 7 becomes,

$$K_i(y_j) = K_{ij} = a_i \frac{p_j}{p_i} \exp \left\{ -\frac{p_j^2}{2p_i^2} \right\}, \quad (8)$$

where $i = 1, 2, \dots, 8$ and $y_i = \ln(p_i) = -4.5, -4, \dots, -1$,

where $j = 1, 2, \dots, 93$ and $y_j = \ln(p_j) = -6.9, -6.8, \dots, 2.3$,

and where a_i normalises K such that $\sum_{j=1}^{93} K_{ij} = 1$.

b. Equation 2 becomes,

$$R_i = \sum_{j=1}^{93} K_{ij} \cdot B(y_0, T_j). \quad (9)$$

The basic temperature profile was obtained using 400 tropical profiles described below. These were interpolated to the 93 levels, y_j , and their mean was used to define the basic state, \underline{T}_0 (a vector of length = 93). This profile was used with equations 8 and 9 to find the radiance in each channel which was then converted to a brightness temperature. The brightness temperatures in all channels are described by a vector (length = 8), \underline{V}_c^i .

To study the effects of a temperature wave, we define a profile,

$$\underline{T} = \underline{T}_0 + \underline{t} \quad , \quad \text{where } t_j = A \sin(k_y y_j + \phi) \quad , \quad (10)$$

and then calculate the corresponding brightness temperatures, \underline{V}^i . By varying the phase of the wave, ϕ , the amplitude of the brightness temperature wave in each channel can be found. This was done for a series of vertical wavenumbers, k_y . Using a temperature wave amplitude, $A = 1$ deg K, the amplitude of the brightness temperature wave then gives a measure of its "attenuation" (relative to the temperature wave producing it). The results are shown in table 1 and figure 2 together with the result for the Gaussian weighting function defined by equation 6.

As expected the variation of attenuation with wavenumber for the Elsasser band weighting functions is similar to that for the Gaussian case. The range of values shown for each k_y represents the variation of attenuation from channel to channel (which results from the non-linearity of the Planck function with respect to temperature). The fact that the radiance wave is attenuated does not necessarily mean that the retrieved temperature wave will be similarly attenuated. This is shown below. However it is to be expected that if the radiance wave is attenuated to the extent that its amplitude falls below the instrumental noise level then the temperature wave cannot be retrieved.

4. Retrieval of a temperature wave using multiple linear regression

The temperature profile estimate, \underline{T}_r , can be retrieved from a measured set of brightness temperatures, \underline{V} , using the regression equation,

$$\underline{T}_r - \underline{\bar{T}} = \underline{\underline{p}} \cdot (\underline{V} - \underline{\bar{V}}) \quad (11)$$

where the regression coefficients are obtained from a "dependent sample" of pairs of \underline{T} and \underline{V} for which $\underline{\bar{T}}$ and $\underline{\bar{V}}$ are the respective means.

Regression coefficients suitable for this study were obtained using a set of 400 tropical temperature profiles selected as being a representative sample (from the NESS set of 1200 atmospheric profiles). Each temperature profile in the sample, \underline{T} , was processed as described above to give brightness temperatures, \underline{V}' . The effect of instrumental noise and other errors in brightness temperature can be included by adding a small random vector to the calculated values:

$$\underline{V} = \underline{V}' + \underline{\epsilon} \quad (12)$$

The regression coefficient matrix, \underline{D} , is then given by,

$$\underline{D} = E \left\{ (\underline{T} - \bar{\underline{T}}) \cdot (\underline{V} - \bar{\underline{V}})^T \right\} \cdot \left(E \left\{ (\underline{V} - \bar{\underline{V}}) \cdot (\underline{V} - \bar{\underline{V}})^T \right\} \right)^{-1}, \quad (13)$$

where E is the expected value operator, and the expected values are obtained using the dependent sample. If the elements of $\underline{\epsilon}$ have zero mean and are uncorrelated then equation 13 becomes.

$$\underline{D} = E \left\{ (\underline{T} - \bar{\underline{T}}) \cdot (\underline{V}' - \bar{\underline{V}}')^T \right\} \cdot \left(E \left\{ (\underline{V}' - \bar{\underline{V}}') \cdot (\underline{V}' - \bar{\underline{V}}')^T \right\} + E \left\{ \underline{\epsilon} \cdot \underline{\epsilon}^T \right\} \right)^{-1}, \quad (14)$$

where $E(\underline{\epsilon} \cdot \underline{\epsilon}^T)$ is a diagonal matrix and the diagonal elements give the square of the brightness temperature noise in each channel.

\underline{D} was calculated from equation 14, i.e. noise-free brightness temperatures were found and a diagonal matrix representing the noise added to the brightness temperature covariance matrix before the matrix inversion operation. This is computationally simpler and more instructive, as it shows how small additions to the diagonal elements of the matrix to be inverted decrease markedly the noise sensitivity of the regression coefficients.

Retrievals were then performed by calculating noise-free brightness temperatures (i.e. $\underline{V} = \underline{V}'$ in equation 11) for the temperature profiles described in section 3 - \underline{T}_0 and $\underline{T} = \underline{T}_0 + \underline{t}$ - and by using a range of values for the following parameters:

- a. The noise, $\underline{\epsilon}$, used in the calculation of regression coefficients. In each case equal values were used for each channel. The values were (brightness temperature noise)² of 0, 0.01, 0.1, 1 and 10 (deg K)².

- b. The vertical wavenumber, k_y . 1, 1.5, 2, 2.5, 3, 3.5 and 4 were used.
- c. The phase of the wave relative to the weighting functions.

If \underline{T}_r and $(\underline{T}_r)_0$ are the retrieved profiles corresponding to the initial profiles \underline{T} and \underline{T}_0 respectively, then the "retrieved wave" is given by

$$\underline{t}_r = \underline{T}_r - (\underline{T}_r)_0 \quad (15)$$

In each case the amplitude of the retrieved wave was compared with the original wave to find the attenuation factor, α , as follows:

$$\alpha = \frac{\sum_j (t_r)_j \cdot t_j}{\sum_j t_j \cdot t_j} \quad (16)$$

As the retrieval can only be expected to be reasonably over the height range in which the weighting functions have significant contributions, in this case $j = 20 \rightarrow 65$, the summations in equation 16 were limited to this region.

The resulting attenuations are shown in table 2 and figure 3. The standard deviations shown represent the changes in attenuation with different phase under the same conditions of brightness temperature noise (in the dependent sample) and vertical wavenumber.

Also of interest is the noise sensitivity of the calculated regression coefficients in each case. Assuming equal noise in all channels, this is given by a noise amplification factor,

$$\beta = \sqrt{\sum_i (D_{ij})^2},$$

where the mean is again computed over the region of the weighting functions, $j = 20 \rightarrow 65$. This is shown in table 3 for each set of regression coefficients.

Conclusions

1. In all cases the waves of lower vertical wavenumber are retrieved with less attenuation. This is as expected and just illustrates the limited vertical resolution of remote soundings of temperature profile.

2. The greater the brightness temperature noise used in the dependent sample, the greater is the attenuation of the retrieved wave for a given wavelength, and the smaller is the sensitivity of the retrieval to noise in the brightness temperatures of the independent measurement.
3. The amplitude of the retrieved temperature wave can be greater than that of the corresponding brightness temperature wave if the noise terms in the regression coefficient calculation are sufficiently low.
4. There is a trade-off between the noise sensitivity and the minimum vertical wavelength which can be retrieved, i.e. the vertical resolution (see figure 4 and c.f. Conrath, 1972).
5. The combined system of radiometer plus retrieval acts as a low-pass filter to the real temperature profile. The attenuation of a given wave is determined principally by the noise on the dependent sample.

Comments

1. If we can reduce the noise on the radiances (instrumental improvements, better cloud-clearing, etc), we can afford to increase the noise sensitivity and thus retrieve waves of shorter wavelength.
2. The noise sensitivity of the retrieval could have been reduced by using stepwise regression rather than a simple multiple regression on all channels. However this method fails to use all the available information and so it also would sacrifice vertical resolution in the retrieved profile.
3. The assumption throughout of waves with a constant amplitude in the vertical is a little unrealistic, particularly in the lower stratosphere where an amplitude increasing with height is often found. However this approximation is not thought to affect the general conclusions.
4. These results are particularly relevant to the study of stratospheric equatorial waves (mixed Rossby-gravity waves and Kelvin waves) which have a vertical wavelength ~ 1 scale height (Holton, 1975). In higher latitudes the dominant standing waves have much larger vertical wavelengths (~ 7 scale heights).

Table 1 Attenuation of brightness temperature wave

Vertical wavenumber k_y	Attenuation of brightness temp. wave			
	Mean	S.D.	Max.	Min.
1	0.60	0.04	0.68	0.55
1.5	0.39	0.03	0.44	0.36
2	0.26	0.02	0.30	0.23
2.5	0.17	0.02	0.21	0.14
3	0.111	0.012	0.129	0.091
3.5	0.076	0.008	0.083	0.060
4	0.052	0.007	0.064	0.043

Table 2 Attenuation of retrieved temperature wave

Values in the table are the mean and standard deviation of the attenuation factor of the retrieved wave.

k_y	(Brightness temperature noise) ² in K ²				
	0	0.01	0.1	1	10
1	1.001	0.999	0.964	0.817	0.475
	.024	.032	.021	.031	.047
1.5	0.966	0.940	0.846	0.548	0.198
	.032	.022	.047	.063	.049
2	0.931	0.898	0.704	0.312	0.064
	.041	.048	.064	.043	.016
2.5	0.891	0.816	0.509	0.155	0.028
	.050	.059	.029	.025	.001
3	0.852	0.635	0.283	0.064	0.012
	.056	.053	.022	.015	.005
3.5	0.793	0.404	0.118	0.020	0.003
	.071	.061	.005	.003	.001
4	0.697	0.207	0.037	0.004	0.000
	.066	.054	.019	.003	.001

Table 3 Sensitivity of the retrieval to noise in the brightness temperatures

Values in the table are for the noise amplification factor.

	(Brightness temperature noise) ² in K ² used in the calculation of the regression coefficients				
	0	0.01	0.1	1	10
Mean	20.6	4.8	2.15	0.96	0.46
S.D.	9.9	1.4	0.47	0.20	0.08

Figure 1

8 Elsassee band weighting functions

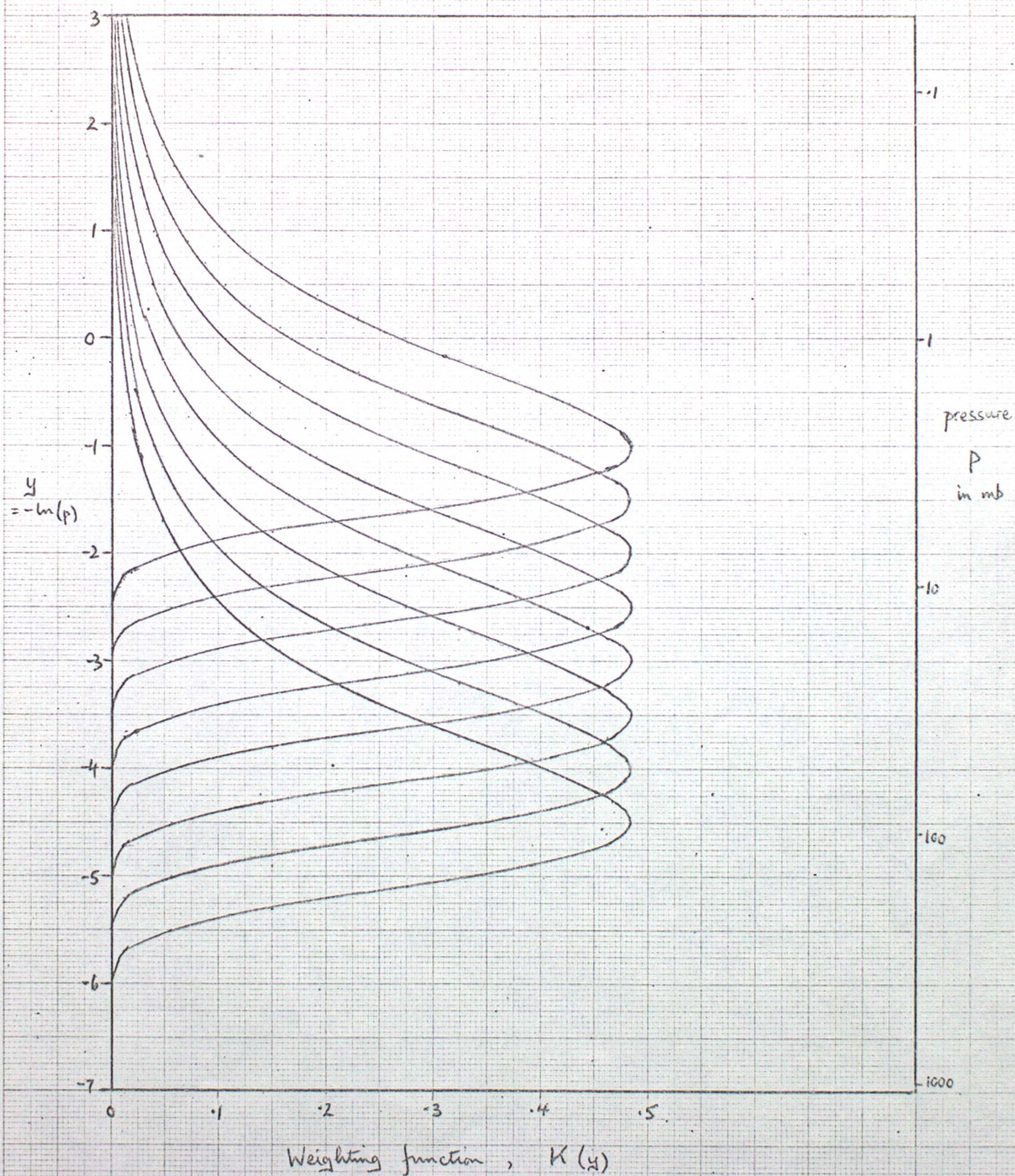


Figure 2

Wave attenuation factor as a function
of vertical wavenumber

Attenuation of brightness temperature wave.

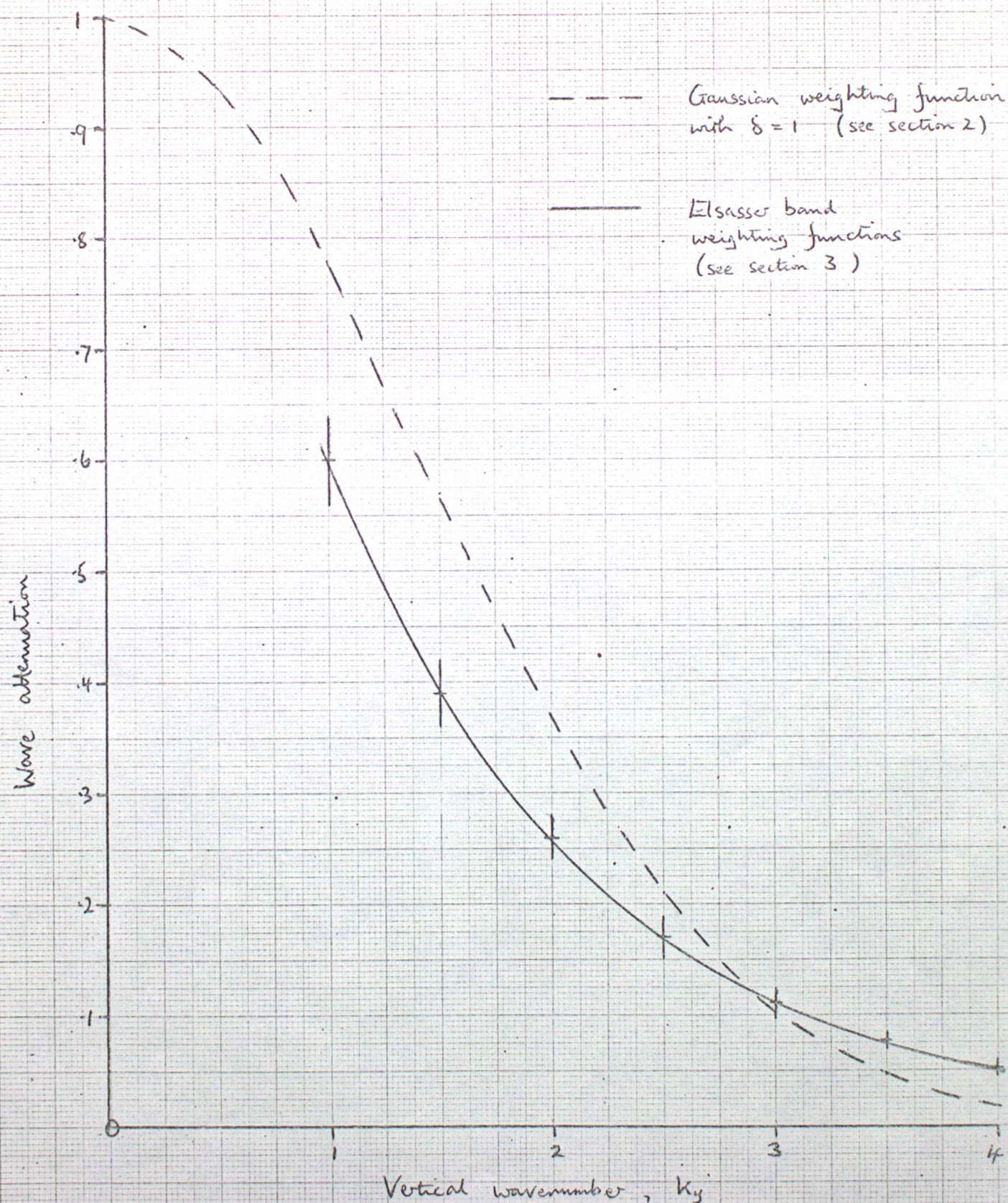


Figure 3

Wave attenuation factor as a function of vertical wavenumber

Attenuation of retrieved temperature wave.

Values on graph are the square of the noise in the brightness temperature used in the calculation of the regression coefficients.

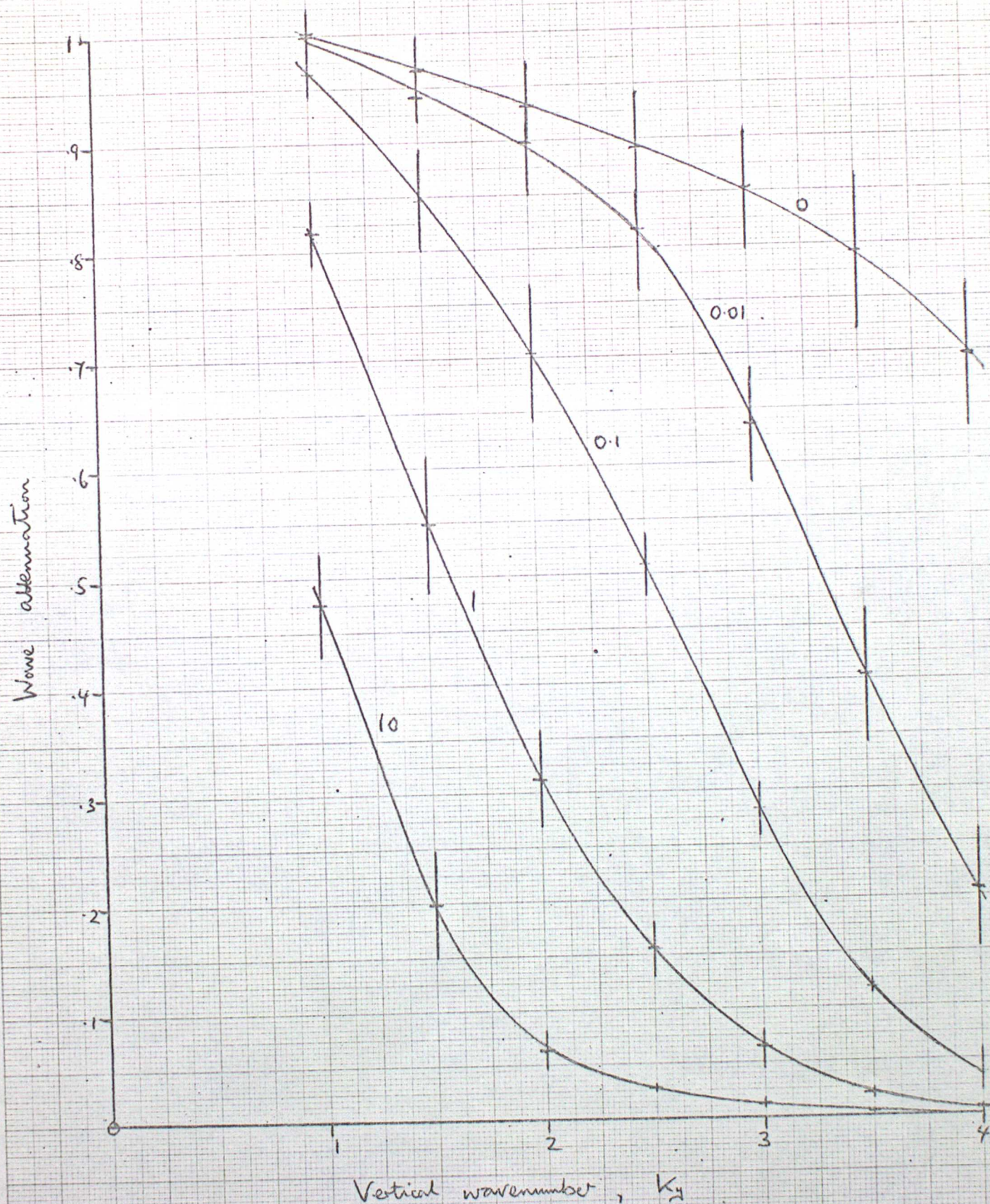
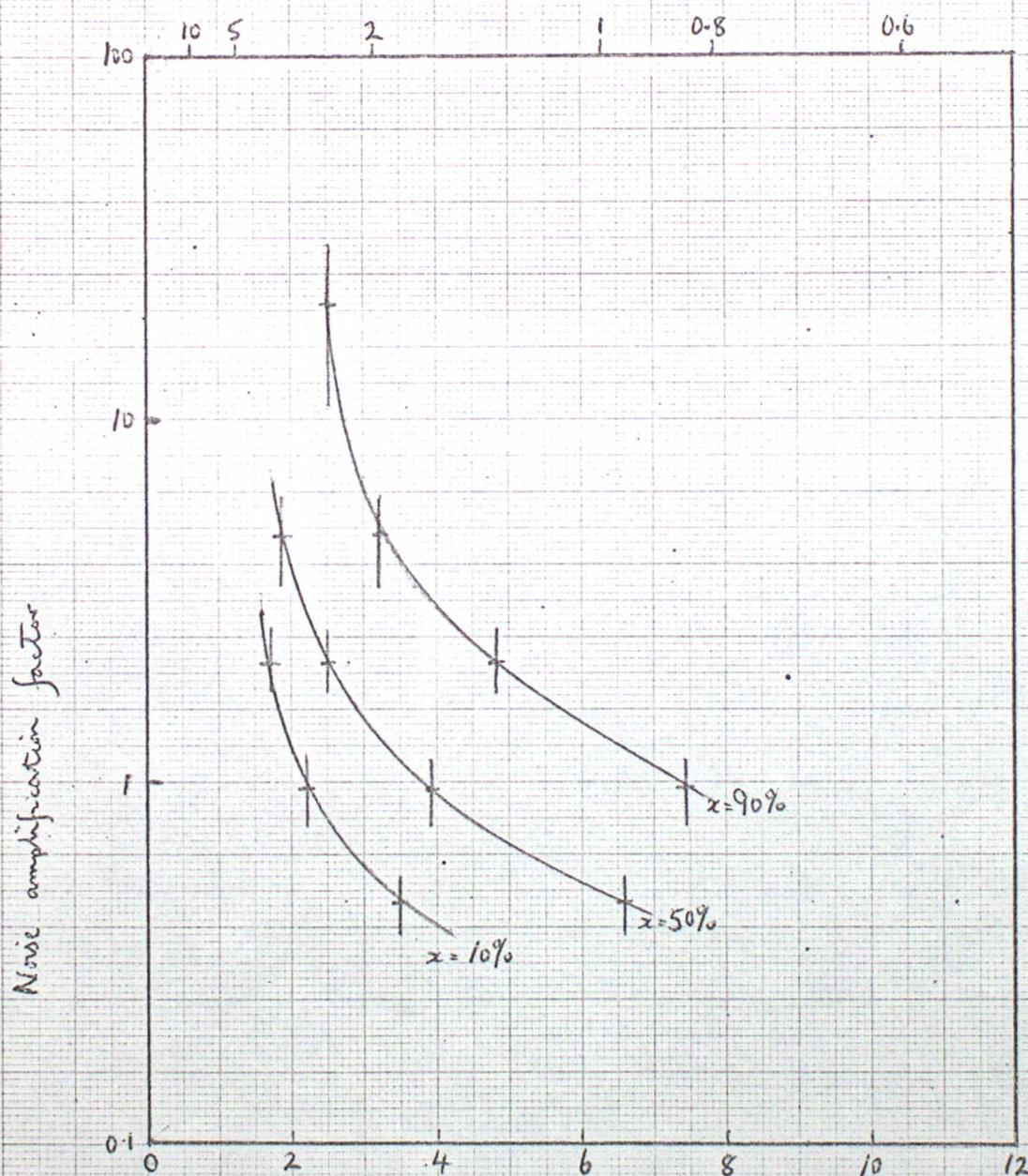


Figure 4

Trade-off between noise sensitivity
and vertical resolution

Maximum wavenumber (in $[\text{scale height}]^{-1}$) for retrieval
of wave at $x\%$ or more of full amplitude



Minimum wavelength (in scale heights) for retrieval
of wave at $x\%$ or more of full amplitude